

# Hydrogel-Based Glucose Sensors: Effects of Phenylboronic Acid Chemical Structure on Response

Chunjie Zhang,<sup>†</sup> Mark D. Losego,<sup>†,‡</sup> and Paul V. Braun<sup>\*,†</sup>

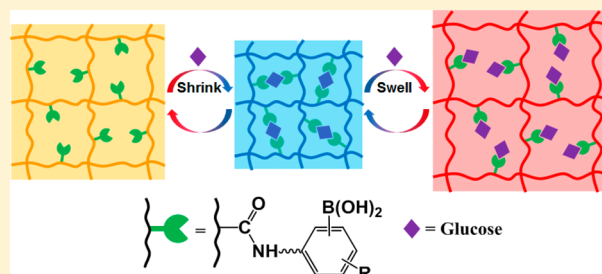
<sup>†</sup>Department of Materials Science and Engineering, Frederick Seitz Materials Research Laboratory, Beckman Institute for Advanced Science and Technology, University of Illinois at Urbana–Champaign, Urbana, Illinois 61801, United States

## S Supporting Information

**ABSTRACT:** Phenylboronic acids (PBAs) are being considered for glucose sensing and controlled insulin release, because of their affinity for diol-containing molecules. The interaction of immobilized PBAs in a hydrogel matrix with glucose can lead to volumetric changes that have been used to monitor glucose concentration and release insulin. Although the interaction of PBAs with diol-containing molecules has been intensively studied, the response of PBA-modified hydrogels as a function of the specific PBA chemistry is not well understood. To understand the interaction of immobilized PBAs with glucose in hydrogel systems

under physiological conditions, the glucose-dependent volumetric changes of a series of hydrogel sensors functionalized with different classes of PBAs were investigated. The volume change induced by PBA-glucose interactions is converted to the diffracted wavelength shift by a crystalline colloidal array embedded in the hydrogel matrix. The PBAs studied contain varying structural parameters such as the position of the boronic acid on the phenyl ring, different substituents on PBAs and different linkers to the hydrogel backbone. The volumetric change of the PBA modified hydrogels is found to be highly dependent on the chemical structure of the immobilized PBAs. The PBAs that appear to provide linear volumetric responses to glucose are found to also have slow response kinetics and significant hysteresis, while PBAs that show nonlinear responses have fast response kinetics and small hysteresis. Electron-withdrawing substituents, which reduce the  $pK_a$  of PBAs, either increase or decrease the magnitude of response, depending on the exact chemical structure. The response rate is increased by PBAs with electron-withdrawing substituents. Addition of a methylene bridge between the PBA and hydrogel backbone leads to a significant decrease in the response magnitude. PBAs with specific desirable features can be selected from the pool of available PBAs and other PBA derivatives with desired properties can be designed according to the findings reported here.

**KEYWORDS:** boronic acid, glucose responsive, hydrogel, sensor, photonic crystal



## 1. INTRODUCTION

Diabetes is a worldwide health concern, with a rapidly increasing diabetic population predicted to reach 366 million by 2030.<sup>1</sup> Intensive research efforts have been devoted to developing glucose monitoring and insulin delivery technologies.<sup>2–9</sup> Glucose responsive hydrogels have been widely studied both as glucose sensors and insulin delivery vehicles.<sup>7,10–12</sup> Typically, binding events of the sensing moieties with glucose can be converted to volumetric changes, which report glucose concentration and, in some cases, directly control the release of insulin.<sup>2,13–15</sup> It is particularly important to understand the sensing moiety interactions with glucose under physiological conditions, and how these interactions impact the absolute magnitude and kinetics of the hydrogel volume change.

Here, we use polymerized crystalline colloidal arrays (PCCA) as facile reporters of the volumetric change of glucose responsive PBA-functionalized hydrogels. PCCAs are a family of colorimetric materials (and, in some cases, sensors) first developed by Asher and co-workers, which consist of a self-organized crystalline colloidal array (CCA) embedded in polymer hydrogel matrix.<sup>16</sup> Unlike inverse opal hydrogels

with highly porous structures, the volumetric change of the hydrogel matrix of a PCCA is more accurately correlated with the diffraction wavelength of the embedded photonic crystal.<sup>17,18</sup> In the PCCA sensors, chemical interactions between the functionalized hydrogel matrix and an analyte induce a volumetric change of the hydrogel. As the hydrogel matrix either expands or shrinks, the lattice spacing of embedded colloidal particles changes, resulting in a wavelength shift of the Bragg diffracted light. With specifically designed hydrogel chemistry, the diffraction wavelength can be used to report the analyte concentration. The lattice spacing of CCA can be tuned anywhere from the UV into the near-IR, enabling in some cases the use of naked eye as the detector.<sup>19</sup> Since only the peak wavelength needs to be determined, not the intensity, interference from the environment is less detrimental, overcoming the loss of accuracy often present in sensors where light intensity, e.g., fluorescence, is used to quantify analyte

Received: May 29, 2013

Revised: July 8, 2013

Published: July 9, 2013



concentration.<sup>20</sup> PCCA sensors have proven to be quite versatile, and have been developed to detect numerous analytes, including metal ions, glucose, alcohol, and pH.<sup>21–25</sup>

Quantitative glucose sensing and controlled insulin release require systems that respond to glucose in a designed and predictable fashion. Rational manipulation of the interactions driving the response enables control of the sensing performance, e.g., sensing range, sensitivity, error, and response rate. We focus on phenylboronic acids (PBAs), which are well-known to have substantial affinities for diol-containing molecules. PBA has high operational stability, in particular compared with glucose oxidase and lectin, which are widely used for glucose sensing.<sup>2,26</sup> Since the discovery of the interactions between PBA and saccharide in 1954, many PBA-based diol sensors have been developed.<sup>27</sup> Although the interaction of PBA derivatives with diols has been intensively studied, the response of PBA-functionalized hydrogel sensors, as a function of the PBA chemistry, is not well-understood. Here, the responses of PBA-based PCCAs, with a focus on the PBA chemistry, were investigated. The glucose concentration range used in our study (0–30 mM) is similar to the concentration range of clinical interest (2.2–38.9 mM).<sup>28</sup> We found systems exhibiting linear responsiveness to glucose also exhibit slow kinetics and significant hysteresis. Electron-withdrawing substituents, which reduce the  $pK_a$  of PBAs do not always lead to increased magnitude of response. Such substituents increase the response kinetics, relative to the PCCAs modified with non-substituted PBAs. Addition of a methylene bridge between the PBA and hydrogel backbone significantly reduces the magnitude of response. Our findings elucidate various aspects of boronic acid chemistry and provide background for new concepts in molecular design of boronic acid-based carbohydrate sensors.

## 2. RESULTS AND DISCUSSION

The PCCAs are chemically attached to glass substrates functionalized with methacryloyl silane, and remain attached during the chemical modification of the hydrogel matrix and glucose sensing tests. This bonding constrains the volume change of hydrogel matrix to the  $z$ -direction; this is important to remember when comparing these results with studies in which the hydrogels change in volume isotropically. Here, the volume change of PCCA is proportional to the change in thickness, which is proportional to the change in lattice constant normal to the substrate of the photonic crystal embedded inside the hydrogel matrix. Thus,  $V/V_0 = h/h_0 = \lambda/\lambda_0$ , where  $V_0$ ,  $h_0$ , and  $\lambda_0$  denote the volume, thickness, and diffraction wavelength of PCCA in the absence of glucose and  $V$ ,  $h$ , and  $\lambda$  denote the same parameters in the presence of glucose.<sup>18,29</sup> Immobilization of the hydrogel enables accurate measurements from the same region of the PCCA over time, and advantageously, the one-dimensional (1D) volume change of the immobilized PCCA results in a larger wavelength shift for a given degree of swelling compared with freestanding PCCA systems, which swell in three dimensions.<sup>30</sup> The specific wavelength of diffracted light can be tuned by changing the concentration of colloids present in the CCA prior to polymerization. The homogeneity of the PCCA structure is evidenced by the narrow distribution of the diffracted wavelength (Figure 1).

After polymerization, the PCCAs were hydrolyzed to provide carboxylic acid sites. Boronation was then performed by soaking the hydrolyzed PCCA in a solution containing an

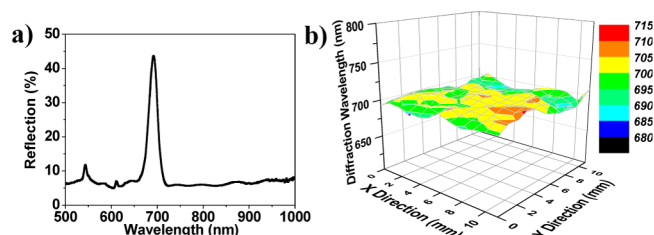


**Figure 1.** (a) Typical reflection spectrum taken from a PBA-modified PCCA using a 10 $\times$  objective lens. (b) A map of the diffraction wavelength over the same PCCA. Measured area, 1.21 cm<sup>2</sup>; number of measured spots, 144; average peak position, 699 nm; standard deviation, 6 nm.

amine-functionalized PBA and the coupling agent EDC (see Scheme 1a).<sup>31</sup> PBAs are categorized into four groups, based on their chemical structures (see Scheme 1b). In Group 1 PBAs, boronic acid is at the ortho position of the amino group on phenyl ring; in Group 2 PBAs, boronic acid is at the meta

**Scheme 1.** (a) Synthetic Route for PBA-Modified PCCAs. (b) PBAs Studied in This Paper

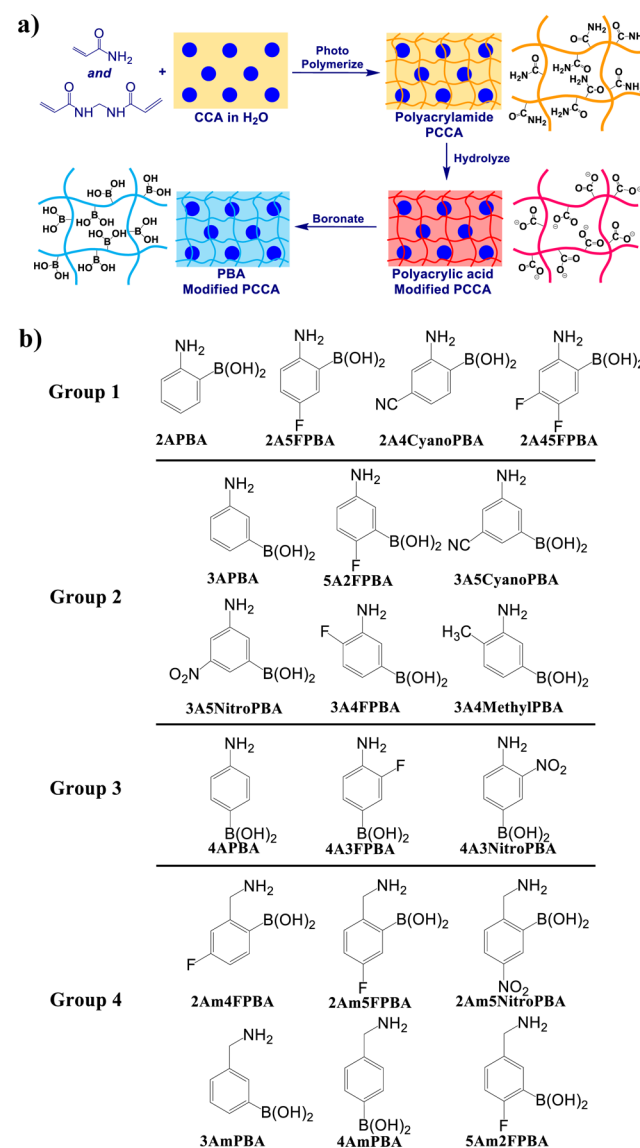


Table 1. Response of PBA-Modified PCCAs in 0–30 mM Glucose Solutions Buffered at pH 7.4 and 37 °C

PBA	hydrolysis time (h)	diffraction order	$\lambda_0$ (nm) <sup>a</sup>	$\Delta\lambda_{10}$ (nm) <sup>b</sup>	$\Delta\lambda_{20}$ (nm) <sup>b</sup>	$\Delta\lambda_{30}$ (nm) <sup>b</sup>	$t_{90}$ (min) <sup>c</sup>
2APBA <sup>e</sup>	16	2	631	−101	−217	−324	>80
2A5FPBA <sup>f</sup>	16	1	980	−146	−309	−435	>65
2A4CyanoPBA	10	1	640	−15	−21	−26	7
2A45FPBA	16	2	731	0	0	0	NA <sup>d</sup>
3APBA	3	1	830	−132	−137	−120	12
5A2FPBA	3	1	1194	−314	−309	−297	6
3A5CyanoPBA	3	1	901	−171	−159	−142	6
3A5NitroPBA	3	1	829	−151	−146	−133	7
3A4FPBA	3	1	924	−105	−113	−101	4
3A4MthylPBA	3	1	856	−25	−28	−22	4
4APBA	3	1	747	−117	−156	−170	16
4A3FPBA	6	1	891	−264	−303	−323	9
4A3NitroPBA	6	2	657	−1	−4	−5	NA <sup>d</sup>
2Am4FPBA	16	1	840	−32	−50	−58	12
2Am5FPBA	16	1	1037	−54	−60	−66	10
2Am5NitroPBA	16	2	612	−24	−24	−24	5
3AmPBA	3	2	663	2	3	5	NA <sup>d</sup>
5Am2FPBA	3	2	651	−6	−6	−8	NA <sup>d</sup>
4AmPBA	3	2	695	1	2	3	NA <sup>d</sup>

<sup>a</sup> $\lambda_0$  is the diffraction wavelength in pH 7.4 physiological buffer at 37 °C. <sup>b</sup> $\Delta\lambda_n = \lambda_n - \lambda_0$ , where  $\lambda_n$  is the diffraction wavelength in  $n$  mM pH 7.4 buffered glucose solution at 37 °C. <sup>c</sup> $t_{90}$  is the time that a PBA-modified PCCA needs to reach 90% of the diffraction wavelength shift from 0–10 mM glucose solution. <sup>d</sup>NA indicates values that cannot be accurately identified. <sup>e</sup>The corresponding PCCA did not reach equilibrium within 2 h for each glucose concentration. <sup>f</sup>The corresponding PCCA did not reach equilibrium within 3 h for each glucose concentration. The  $t_{90}$  was calculated using data within 2 h of testing.

position of the amino group; in Group 3 PBAs, boronic acid is at the para position; in Group 4 PBAs, aminomethyl groups are present, instead of amino groups. In all cases, the PBA is linked by an amide bond formed by reacting the amino groups on the PBAs with carboxylates in the hydrolyzed PCCAs. To achieve a substantial diffraction wavelength shift over the glucose concentration range of interest (0–30 mM), various PBA loadings are necessary due to the variations in PBA binding constants with glucose and their capability to change the volume of hydrogel matrix upon binding. The PBA loading was varied by changing the hydrolysis time (see Table 1 and Table S1 in the Supporting Information). The final diffraction wavelength of the PBA-modified PCCA depends on both the PBA loading and the PBA chemistry (Table 1). Both first- and second-order diffraction peaks ( $m = 1, 2$  in the relationship  $m\lambda = 2nd \sin \theta$ ) were used to monitor glucose concentration. For example, for the 2APBA-modified PCCA, the second order diffraction peak ( $m = 2$ ) was used for detecting 0–10 mM glucose as the negative charge on the immobilized 2APBA moieties makes them hydrophilic at pH 7.4, resulting in a swollen hydrogel matrix, putting the first-order peak at zero glucose concentration in the infrared (out of the range of our detector), and the second-order peak in the visible region.

The immobilized PBAs reversibly bind with diols in glucose, forming either a 1:1 complex or a 2:1 cross-linking complex between PBA and glucose (Figure 2).<sup>32</sup> The PBA-glucose complex has a lower  $pK_a$  than the corresponding PBA,<sup>20,33</sup> and thus the concentration of anionic boronate species in the PCCA increases upon binding with glucose. As shown in Figure 3, when glucose concentration is lower than a critical level, the 2:1 cross-linking complex is preferentially formed, leading to additional crosslinks in the PCCA, resulting in contraction of the hydrogel matrix and a blue shift of the diffracted light. As the glucose concentration increases, the 2:1 complex is converted to two 1:1 complexes. As this happens, the number

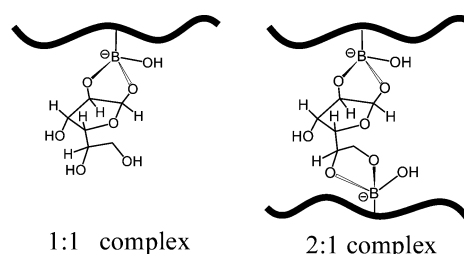


Figure 2. Schematics of the 1:1 complex and 2:1 complex formed between immobilized PBAs and glucose.  $\alpha$ -D-Glucopyranose is used to represent glucose in this paper.

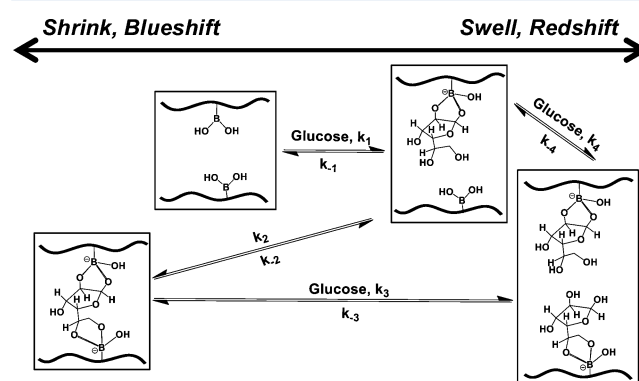
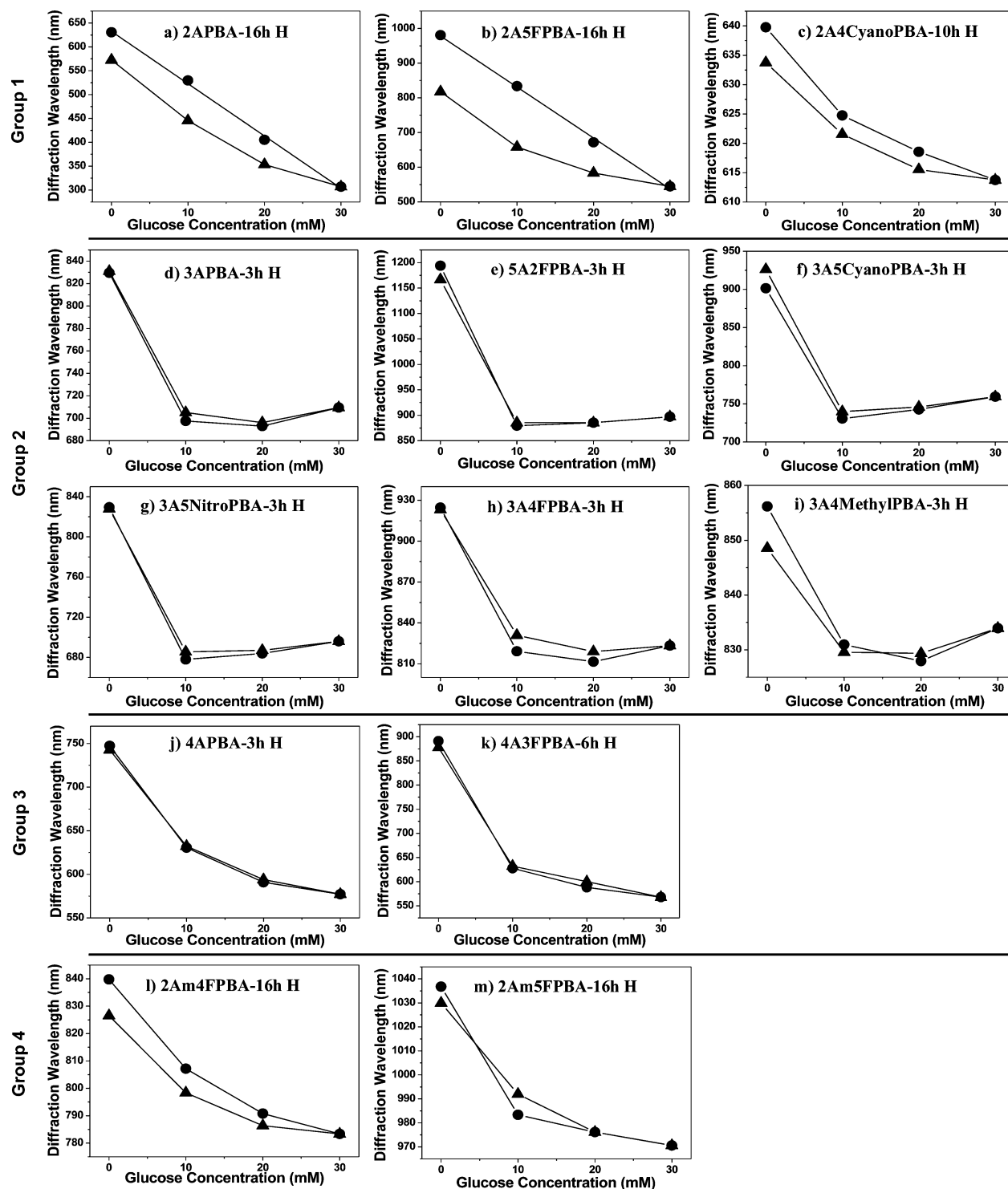


Figure 3. Interactions of PBA-modified hydrogel with glucose and the effect on the hydrogel volume and diffraction wavelength of PCCA.

of crosslinks decreases, and the number of free anionic 1:1 complexes increases. The reduction in cross-link density and increase in charged species lead to an expansion in the hydrogel volume, which redshifts the wavelength of diffracted light.

To test the response of the PBA-modified PCCAs, we varied the glucose concentration from 0 to 30 mM back to 0 mM in



**Figure 4.** Diffraction wavelength during increasing (●) and decreasing (▲) glucose concentration for PCCAs modified with (a) 2APBA, (b) 2A5FPBA, (c) 2A4CyanoPBA, (d) 3APBA, (e) 5A2FPBA, (f) 3A5CyanoPBA, (g) 3A5NitroPBA, (h) 3A4FPBA, (i) 3A4MethylPBA, (j) 4APBA, (k) 4A3FPBA, (l) 2Am4FPBA, and (m) 2Am5FPBA. For the ease of reading, the specific PBA and hydrolysis time (in hours) are denoted as “PBA-*n*h H” inside each figure. All tests were performed in pH 7.4 buffered glucose solutions at 37 °C. The lines in panels (a) and (b) for increasing glucose concentrations are linear fits; other lines are aids to the eye.

10 mM steps at 37 °C. The hysteresis during cycling can be observed as the difference in diffraction wavelength for the decreasing glucose concentration sweep, relative to the increasing concentration sweep for a given glucose concentration. For sensors, minimal hysteresis over the glucose concentration range of interest is desirable. The detailed

diffraction wavelength changes and response curves of the PBA modified PCCAs to glucose are summarized in Table 1 and Figure 4, respectively.

**Glucose Sensing of PBA-Modified PCCAs.** As shown in Figures 4a and 4b, PCCAs containing 2APBA and 2A5FPBA (Group 1) exhibit a nearly linear response with an overall



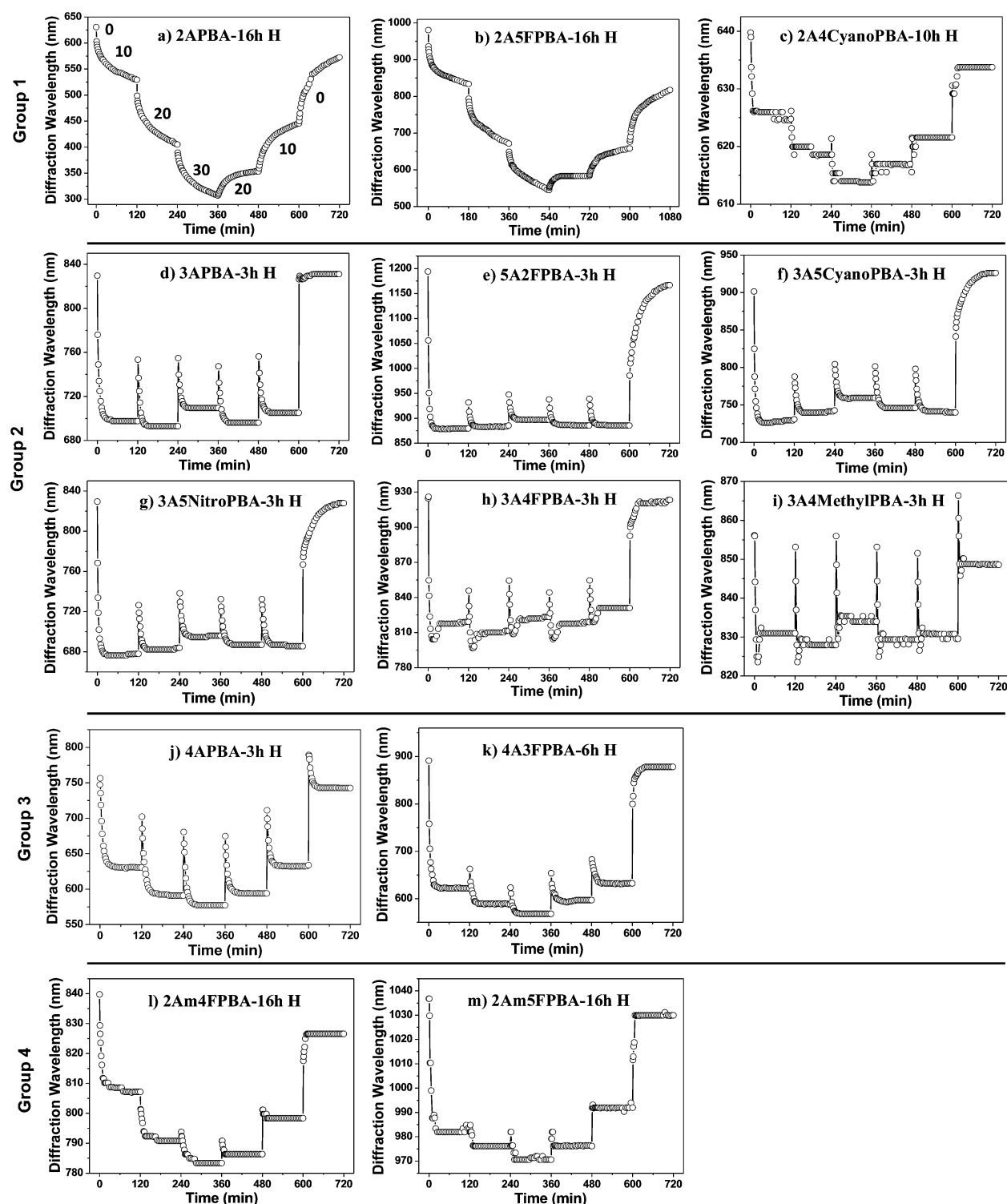


**Figure 5.** Response kinetics of PCCAs modified with (a) 2APBA, (b) 2A5FPBA, (c) 2A4CyanoPBA, (d) 3APBA, (e) 5A2FPBA, (f) 3A5CyanoPBA, (g) 3A5NitroPBA, (h) 3A4FPBA, (i) 3A4MethylPBA, (j) 4APBA, (k) 4A3FPBA, (l) 2Am4FPBA, and (m) 2Am5FPBA in pH 7.4 buffered glucose solutions stepping from 0 to 30 mM back to 0 mM glucose at 37 °C (steps labeled in panel (a)). The PBA and hydrolysis time (in hours) are denoted as “PBA-*nh* H” inside each figure. Lines connecting data points serve as an aid to the eye.

wavelength shift of more than 300 nm over 0–30 mM glucose and a significant hysteresis. We ascribe the blue shift to the shrinkage in hydrogel volume caused by the formation of the 2:1 complex (Figure 3). As can be seen from Figures 5a and 5b, both 2APBA- and 2A5FPBA-modified PCCAs exhibit slow response kinetics and do not reach equilibrium at each glucose

concentration step. Focusing only on the 2APBA system, as expected, the overall diffracted wavelength shift of 2APBA-modified PCCA in 0–30 mM glucose can be tuned by varying the hydrolysis time during the chemical modification. As the hydrolysis time increases, more carboxylate sites are generated for PBA attachment and therefore a larger wavelength shift is

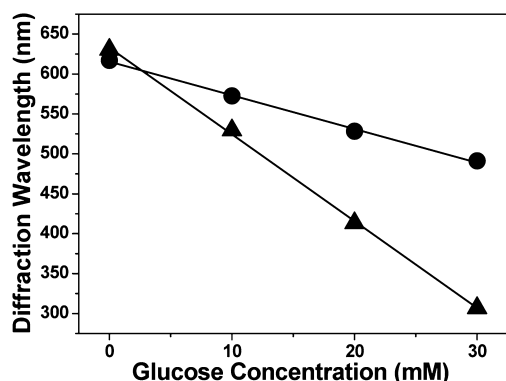


**Figure 6.** Diffraction wavelength (second order) versus glucose concentration for 2APBA-modified PCCAs after (●) 8 h of hydrolysis and (▲) 16 h of hydrolysis. Tests were performed in pH 7.4 buffered glucose solutions at 37 °C. Lines are linear fits.

observed for a given glucose concentration change. As shown in Figure 6, after an 8-h hydrolysis, the 2APBA-modified PCCA exhibits an  $\sim 130$  nm shift while after 16 h of hydrolysis, the wavelength shift is  $\sim 300$  nm. This may be useful for tailoring the sensitivity and dynamic range of glucose responsive PCCAs. Despite being in the same group as 2APBA and 2A5FPBA, the 2A4CyanoPBA-modified PCCA shows fast response kinetics, a nonlinear response, and a decreased sensitivity above 10 mM glucose (see Figures 4c and 5c). Finally, the PCCA modified with 2A45FPBA (also Group 1) shows no response to glucose (see Table 1).

PCCAs modified by Group 2 PBAs generally exhibit a blue shift with increasing glucose up to some critical concentration. The 3APBA-modified PCCA shows a blue shift below 20 mM glucose (Figure 4d). However, when the glucose concentration exceeds  $\sim 20$  mM, a red shift is observed. This nonlinear response indicates that the 2:1 complex formed below 20 mM glucose significantly shrinks the hydrogel, while above 20 mM glucose, the formation of the 1:1 complex leads to an expansion in the hydrogel volume (Figure 3). The 3APBA-modified PCCA shows a large response under physiological conditions while in previous reports, 3APBA-modified PCCAs only show a relatively small response at high pH values.<sup>32</sup> Other Group 2 PBAs have similar response curves, except that 5A2FPBA-, 3A5CyanoPBA-, and 3A5NitroPBA-modified PCCAs start red-shifting when the glucose concentration exceeds  $\sim 10$  mM rather than 20 mM (see Figures 4e–g). The 4APBA- and 4A3FPBA-modified PCCAs (Group 3) also have nonlinear response curves (see Figures 4j and 4k). The sensitivity of these PCCAs decreases when the glucose concentration exceeds 10 mM, although no red shift is observed. The 4A3FPBA-modified PCCA in our study shows a significantly larger response under physiological conditions than prior work,<sup>32</sup> even without polyethylene glycol moieties used in that work to stabilize the PBA–glucose complexes, possibly because of the high 4A3FPBA concentration in our hydrogel matrix. The Group 3 4A3NitroPBA-modified PCCA shows almost no response to glucose, as shown in Table 1.

The Group 4 PBAs have aminomethyl groups instead of amino groups as in Groups 1–3. Group 4 PBA-modified PCCAs show a considerably smaller wavelength shift than Group 1–3 PBA-modified PCCAs, as can be seen by comparing 2Am5FPBA- and 2A5FPBA-, 3AmPBA- and 3APBA-, 4AmPBA- and 4APBA-, 5Am2FPBA- and 5A2FPBA-modified PCCAs. 2Am4FPBA- and 2Am5FPBA-

modified PCCAs exhibit nonlinear sensing curves, with a decreased sensitivity above  $\sim 10$  mM glucose (see Figures 4l and 4m). The 2Am5NitroPBA-modified PCCA has only a small response to glucose below 10 mM, and it loses sensitivity as the glucose concentration exceeds  $\sim 10$  mM (Table 1). PCCAs modified by 3AmPBA, 4AmPBA, and 5Am2FPBA show almost no response to glucose, as indicated in Table 1. Unlike the Group 1 PBAs, which exhibited a significant hysteresis, no obvious hysteresis was observed for PCCAs modified with Group 2–4 PBAs.

Fast response kinetics is an important attribute for glucose monitoring, and, in particular, continuous glucose monitoring.<sup>4</sup> PCCAs modified with Group 2 PBAs all show fast response kinetics (see Figures 5d–i). For Group 3 systems, the 4APBA- and 4A3FPBA-modified PCCAs show slower response kinetics, compared to 3APBA and 3A4FPBA in Group 2 (Figures 5j and 5k). The PCCAs modified with 2Am4FPBA and 2Am5FPBA (Group 4) exhibit fast response kinetics (Figures 5l and 5m). As previously discussed, Group 1 PBAs exhibit both slow and fast response kinetics, depending on the substituents on the PBA.

**Rate-Limiting Parameters in Response Kinetics.** The response kinetics of the PBA-modified PCCAs are a convolution of at least two processes: diffusion of glucose into the PBA-modified hydrogel matrix and PBA–glucose reactions. To investigate the rate-limiting step, the thickness of the PBA-modified PCCAs was varied between 30  $\mu\text{m}$  and 120  $\mu\text{m}$ , which represents changes in the glucose diffusion distance. The response kinetics were then recorded for a 0–10 mM glucose concentration step. As shown in Figures 7a and 7b,

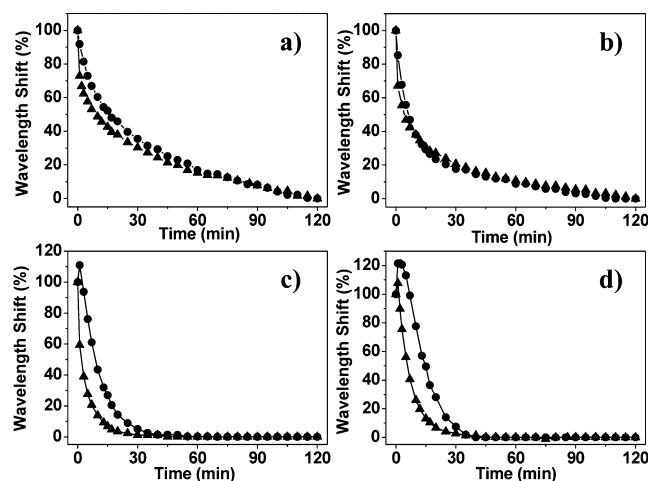


**Figure 7.** Response kinetics of (▲) 30- $\mu\text{m}$ -thick and (●) 120- $\mu\text{m}$ -thick PCCAs modified with (a) 2APBA, (b) 2A5FPBA, (c) 3APBA, and (d) 4APBA from 0 to 10 mM pH 7.4 buffered glucose solutions at 37 °C. Wavelength shift is normalized as  $100 \times (\lambda - \lambda_{\min}) / (\lambda_{\max} - \lambda_{\min})$  (%), where  $\lambda$  is the diffraction wavelength at a specific time, and  $\lambda_{\max}$  and  $\lambda_{\min}$  are, respectively, the highest and lowest wavelengths observed. The lines connecting data points are in place to aid the eye.

both the 2APBA- and 2A5FPBA-modified PCCAs exhibit similar slow response kinetics without reaching equilibrium within 2 h of testing. Thirty-micrometer (30- $\mu\text{m}$ )-thick PCCAs do not exhibit significantly faster response rates than 120- $\mu\text{m}$ -thick PCCAs, indicating that glucose diffusion is not rate-limiting. In Figures 7c and 7d, it can be seen that 3APBA- and 4APBA-modified PCCAs reach equilibrium within  $\sim 40$  min,

which is much faster than the equilibration time of the 2APBA- and 2A5FPBA-modified PCCAs. The 30- $\mu\text{m}$ -thick PCCAs respond faster than the 120- $\mu\text{m}$ -thick PCCAs, indicating that glucose diffusion kinetics substantially contribute to the response rate. This also suggests that the reactions of glucose with the immobilized 3APBA and 4APBA are relatively rapid, compared to the binding of glucose with the immobilized 2APBA and 2A5FPBA. Since all PCCAs have identical hydrogel backbones and similar water volume fractions, the kinetics of glucose diffusion are similar across the PCCA systems.

**PBA-Dependent Response Mechanisms.** The diffracted wavelength shift of the PBA-modified PCCAs upon glucose addition is a function of the volume change of the hydrogel matrix caused by the glucose-induced change in cross-link and charged species density.<sup>16,18</sup> The number of cross-links and charged species formed due to the interactions of glucose with PBA is dependent on the specific PBA chemistry. Thus, the response of the PBA-modified PCCAs enables study of the interactions between immobilized PBAs and glucose. 2APBA- and 2A5FPBA (Group 1)-modified PCCAs show linear and slow responses to 0–30 mM glucose, which are different from PBAs in Groups 2–4 (see Figures 4 and 5). Here, we use the Group 1 2APBA-modified PCCA as an example to discuss the response mechanism and contrast it to that of the Group 2 3APBA-modified PCCA (one of the fast and nonlinear systems). In the hydrogel matrix, for 2APBA, a heterocyclic ring is formed by an intramolecular B–O bond between the boron atom and amide linkage located at the ortho position (see Figure S1a in the Supporting Information).<sup>34</sup> To confirm the formation of the B–O bond, Raman spectroscopy was performed on polyacrylamide (PAAm) thin films functionalized with different PBAs after 70 h of hydrolysis (Figure 8a). In

contrast to other PBAs, the carbonyl peak of immobilized 2APBA appears at a lower wavenumber (increased bond length), indicating the formation of the heterocyclic ring between the carbonyl and the vicinal boronic acid. The same trend is observed on 2AcePBA, 3AcePBA, and 4AcePBA (chemical structures shown in Figure S2 in the Supporting Information), the acetic acid derivatives of 2APBA, 3APBA, and 4APBA, which represent the immobilized PBA moieties inside the hydrogel (Figure 8b).

We ascribe the small, linear, and slow response of 2APBA-modified PCCA to the heterocyclic structure formed on the immobilized 2APBA moieties, which leads to low reactivity toward glucose. To evaluate the reactivity of immobilized PBAs with glucose, Alizarin Red S (ARS), which contains a pair of vicinal diols was used as an indicator for UV–vis spectroscopy measurements (see Figure S2 in the Supporting Information). Upon mixing with 3AcePBA and 4AcePBA, ARS showed an instant color change from red to orange and the absorbance spectra remained the same over the 2 h of monitoring (Figure 9a), indicating the fast reaction kinetics of ARS with 3AcePBA

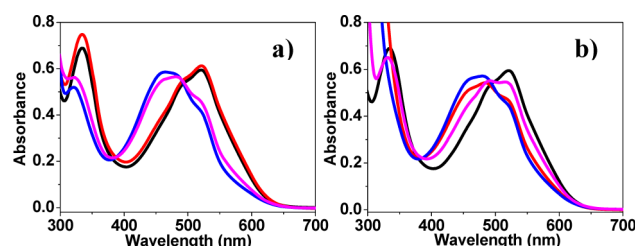


**Figure 9.** UV–vis spectra of 0.1 mM ARS with 1.0 mM PBAs in pH 7.4 buffer at 20 °C: (a) 0.1 mM ARS (black), ARS with 2AcePBA (red), 3AcePBA (blue), and 4AcePBA (magenta); (b) 0.1 mM ARS (black), ARS with 2APBA (red), 3APBA (blue), and 4APBA (magenta).

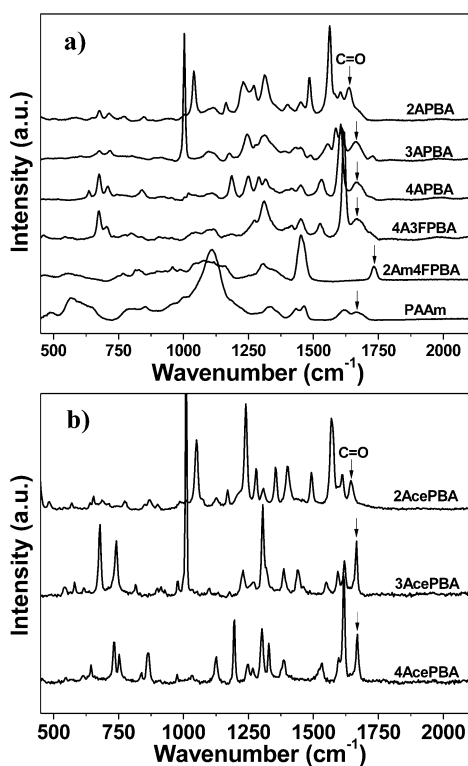


**Figure 8.** Raman spectra of (a) PBA-modified PAAm films, the PBA used for functionalizing the PAAm film is indicated on each spectrum, and (b) three different AcePBAs.

and 4AcePBA. However, the absorbance spectrum of ARS mixed with 2AcePBA remained almost the same as the ARS spectrum even after 2 h, suggesting that 2AcePBA has a low reactivity with ARS. Interestingly, 2APBA, 3APBA, and 4APBA all rapidly react with ARS (Figure 9b). The low reactivity of 2AcePBA with ARS can be ascribed to the heterocyclic ring formed between the carbonyl and its neighboring boronic acid. Obviously, the carbonyl in either 3AcePBA or 4AcePBA does not affect the reactivity toward ARS.

In 2APBA-modified PCCA, the boron atom is negatively charged at physiological pH, which is, in contrast, to the 3APBA-modified PCCA, where the boron atom is neutral. Therefore, at pH 7.4, the 2APBA-modified PCCA is swollen relative to the 3APBA-modified PCCA. This agrees with the fact that the diffracted wavelength of 2APBA-modified PCCA is red-shifted, relative to the diffraction peak of the 3APBA-modified PCCA. Upon exposure to glucose, the immobilized 2APBA forms 2:1 complex, leading to a blue shift of the diffracted light.<sup>35</sup> Once formed, it is difficult for free glucose to break this complex into 1:1 complexes (Figure 3). Therefore, no red shift is observed during the increase of glucose concentration, quite unlike the response of the 3APBA-modified PCCA (see Figures 4a and 4d). As shown in Table 1 and Table S1 in the Supporting Information, the concentration of 2APBA in its corresponding PCCA is much higher than that of the 3APBA-modified PCCA due to the much longer hydrolysis time during the chemical modification.



To rule out effects induced by the difference in PBA content, a 2APBA-modified PCCA using a 3-h hydrolysis, the same hydrolysis time as the 3APBA-modified PCCA, was tested. For both 3 and 8 h of hydrolysis time, a linear response was observed from 0 to 30 mM glucose (Figure 10). As the glucose

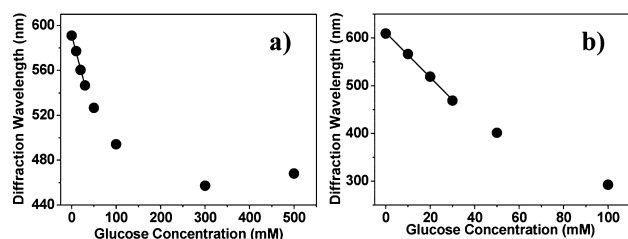


**Figure 10.** Diffraction wavelength (second order) versus glucose concentration for 2APBA-modified PCCAs after (a) 3 h of hydrolysis and (b) 8 h of hydrolysis. Measured in pH 7.4 buffered glucose solutions at 37 °C. Data points from 0 to 30 mM glucose are linearly fitted. Samples were allowed to sit for 2 h at each concentration.

concentration is further increased, the diffracted wavelength of the 3-h hydrolyzed sample gradually deviates from linearity, and when the glucose concentration exceeds 300 mM, the diffracted wavelength starts to red shift, which is caused by the dissociation of 2:1 complex (Figure 10a). The trend of blue shift at low glucose concentration and red shift at high glucose concentration is similar to that of the 3APBA-modified PCCA, however, the critical concentration where the diffracted wavelength starts to redshift is much higher for 2APBA-modified PCCAs, indicating the 2:1 complex is more stable in the 2APBA system than the 3APBA system. For 2APBA, dissociation of the 2:1 complex by glucose is unfavored, perhaps due to the steric hindrance around the boron atoms in this complex.

We believe the large hysteresis of the 2APBA-modified PCCA is a result of the slow kinetics of the 2APBA–glucose interactions, and is not inherent to the hydrogel matrix, because there is minimal hysteresis in the 3APBA system, which is based on the same hydrogel. For 3APBA-modified PCCA, when glucose is below 20 mM, the 2:1 complex formation results in a blue shift of the diffracted light. As the glucose concentration exceeds 20 mM, the 1:1 complex increases, generating more free anionic species, which leads to swelling, and a red shift of the diffracted light (Figure 4d). We believe that the cause of nonlinear response of the Group 2–3 PBA-modified PCCAs is that the concentrations of 2:1 and 1:1 complexes are not proportional to glucose concentration. The fast response and small hysteresis for these PCCAs indicate that (i) the kinetics for formation and dissociation of both the 2:1 and 1:1 complexes are rapid, relative to the glucose diffusion kinetics, and (ii) all these systems probably follow similar mechanisms.

When the glucose concentration suddenly increases, for example, from 10 to 20 mM, the formation of 1:1 complexes leads to an expansion of the hydrogel volume, which is typically observed as a spike on the kinetics curves of PCCAs modified by Group 2–3 PBAs (see Figures 5d–k).  $k_1$ ,  $k_3$ , and  $k_4$  in Figure 3 may all contribute to the abrupt redshift. The 1:1 complex formed through  $k_1$  gradually reacts with the free 3APBA moieties via  $k_2$ , generating the 2:1 complex that shrinks the hydrogel. The diffracted wavelength then blue-shifts until it reaches equilibrium. The abrupt red shift from 0 to 10 mM glucose also exists but is hard to observe, because  $k_2$  is fast enough to generate the quantity of 2:1 complex needed to

shrink the hydrogel. When glucose concentration is decreased, an instantaneous red shift is observed, followed by a blue shift that leads to equilibrium. The abrupt red shift can be caused by the fast dissociation of 2:1 complex via  $k_{-2}$ . The quantity of crosslinks inside the hydrogel decreases and anionic 1:1 complex is generated, leading to the expansion in hydrogel volume. The anionic 1:1 complex then dissociates over time via  $k_{-1}$  and generates neutral boronic acid;  $k_{-4}$  also leads to the decrease in anionic species, resulting in the blue shift of diffracted light. The abrupt red shift becomes less significant when tested at room temperature indicating that temperature also has a contribution at 37 °C. Since the concentrations of all species are unknown within the hydrogel, we are not able to determine the rate and equilibrium constants. Interestingly, no abrupt red shift is observed on the kinetics curves of 2APBA- and 2A5FPBA-modified PCCAs at both room temperature and 37 °C. As there is no net charge difference during the 1:1 complex formation, these PCCAs do not undergo volume expansion (the mechanism for the abrupt red shift in the 3APBA and 4APBA systems).

**Substituent-Response Diagram.** To compare the wavelength shift of PCCAs modified with different PBAs after a given hydrolysis time, we functionalized the PCCAs after 3 h of hydrolysis. The wavelength change for a 0–10 mM glucose step is summarized in Figure 11. For Group 1, the PCCA modified

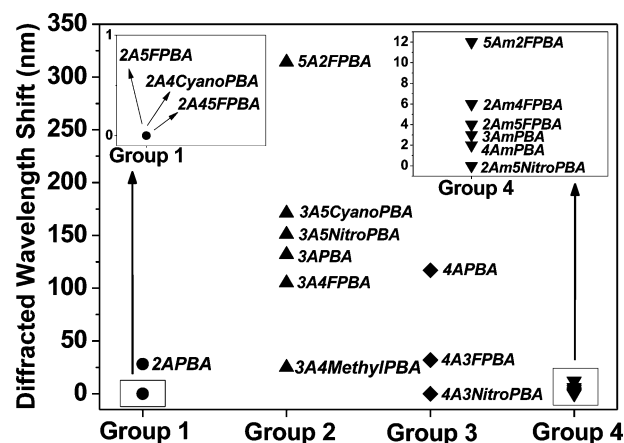


**Figure 11.** First-order diffraction wavelength shift of the 3-h-hydrolyzed PCCAs modified with Group 1–4 PBAs from 0 to 10 mM glucose in pH 7.4 buffer at 37 °C. The inset shows the Group 1 and Group 4 PBA-modified PCCAs.

with 2A5FPBA, which has an electron-withdrawing fluorine substituent, shows less wavelength shift than 2APBA-modified PCCA. This indicates introducing electron-withdrawing substituents on Group 1 PBA reduces the wavelength shift. For PBAs in Group 2, electron-withdrawing substituents can either increase or decrease the wavelength shift. 5A2FPBA-modified PCCA has the largest wavelength shift, because of the strong inductive effect of the vicinal fluorine substituent. When the electron-withdrawing group moves to the meta position, as in 3A5CyanoPBA and 3A5NitroPBA, the inductive effect decreases and therefore the wavelength shift is smaller than the 5A2FPBA-modified PCCA but still larger than 3APBA-modified PCCA. Although nitro groups are more electronegative than cyano groups, the wavelength shift of 3A5NitroPBA-modified PCCA is less than 3A5CyanoPBA-modified PCCA. 3A4MethylPBA, which has an electron-donating methyl



group, leads to a decreased wavelength shift, compared to 3A4FPBA. This can be ascribed to the reduced reactivity of boronic acid, because of the electron-donating groups. For Group 3, electron-withdrawing groups reduce the wavelength shift of the corresponding PCCAs, as can be seen by comparing 4APBA-, 4A3FPBA-, and 4A3NitroPBA-modified PCCAs. All Group 4 PBA-modified PCCAs show small wavelength shift. Increasing the electronegativity of substituents on Group 4 PBAs decreases the wavelength shift, as indicated by 2Am5FPBA- and 2Am5NitroPBA-modified PCCAs. 5Am2FPBA-modified PCCA shows higher wavelength shift than 3AmPBA-modified PCCAs, because of the inductive effect by the ortho fluorine substitute. As can be seen from the response kinetics of PCCAs modified with Group 1–3 PBAs, introducing electron-withdrawing substituents on PBAs increases the response rate.

#### Effects of Charged Species on Volumetric Changes.

The concentration change of charged species upon glucose binding is a key factor that determines the response. The order of diffraction peaks used for detecting glucose concentrations and the starting wavelength at 0 mM glucose are correlated with the concentration of the charged species inside the hydrogel matrix. Therefore, it is important to study the change of charged species in PBA-modified PCCAs to understand the diffraction wavelength shift during glucose monitoring. The volume change of a PBA modified hydrogel matrix induced by a pH change is directly expressed as diffracted wavelength shift, which reports the change in charged species.

The volume change of PBA-modified PCCAs during pH titration can be categorized into two groups, which are summarized in Figure 12. As shown in Figure 12a, the

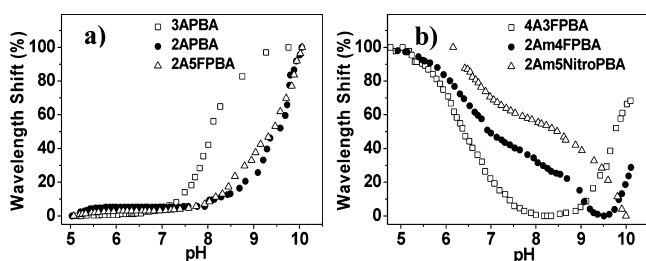


**Figure 12.** Normalized diffraction wavelength shift as a function of pH for PCCAs modified with (a) 3APBA, 2APBA, and 2A5FPBA and (b) 4A3FPBA, 2Am4FPBA, and 2Am5NitroPBA. Tests were performed at 20 °C. Normalized diffraction wavelength shift =  $100 \times (\lambda - \lambda_{\min}) / (\lambda_{\max} - \lambda_{\min})$  %, where  $\lambda$  is the diffraction wavelength at a specific pH value, and  $\lambda_{\max}$  and  $\lambda_{\min}$  are the highest and lowest wavelength during the pH titration, respectively.

3APBA-modified PCCA exhibits a red shift, starting from pH 7.0, which is due to the increase in anionic boronate ion of the immobilized 3APBA moieties (see Figure S1b in the Supporting Information). As the pH increases from 5.0 to 7.0, the diffracted wavelength red-shifts only slightly, indicating a trivial increase in the concentration of anionic boronate ions. The diffraction wavelength of 2APBA-modified PCCA remains almost constant in pH 6.0–8.0. This is believed to result from the anionic heterocyclic ring, which is the dominant species in this pH range. As pH exceeds 8.5, the heterocyclic ring starts to open, generating acyclic boronate ions of 2APBA, leading to a significant red shift of the diffracted wavelength (see Figure S1a in the Supporting Information). The titration results of 3APBA- and 2APBA-modified PCCAs are in agreement with previous

reports.<sup>34,36</sup> The 2A5FPBA-modified PCCA shows a titration curve similar to that of the 2APBA-modified PCCA, except there is a slow increase in diffracted wavelength from pH 6.0 to pH 8.0. In contrast to the red shift in Figure 12a, 4A3FPBA-, 2Am4FPBA-, and 2Am5NitroPBA-modified PCCAs show decreased diffracted wavelength during the increase of pH (Figure 12b). The fluorine and nitro substituents are likely to form hydrogen bonds with protons at low pH,<sup>37–39</sup> generating positive charges on the immobilized PBAs, which lead to a swollen state of the hydrogel matrix. As the pH increases, the amount of positive charges decreases, because of the decrease in proton concentration, which leads to the shrinkage of the hydrogel matrix. In the meanwhile, the neutral boronic acid inside the hydrogel is converted to anionic boronate ion, which first neutralizes the positive charges and shrinks the hydrogel matrix, and then leads to an expansion of hydrogel volume by increasing anionic species. The substituent and boronic acid both contribute to the volume change of the hydrogel matrix during pH titration, leading to trends different from 3APBA-modified PCCAs. The 4A3FPBA- and 2Am4FPBA-modified PCCAs are relatively less swollen at pH 7.4, so that the first-order diffraction peaks were used for the glucose sensing test, while the 2Am5NitroPBA-modified PCCA is more swollen at pH 7.4, therefore, only the second-order diffraction peak was tracked by the detector.

Since the electron-withdrawing substituents on PBAs can immobilize positively charged species via hydrogen bonding, a positive charge background may exist at pH 7.4, which complicates the charge state of the hydrogel matrix upon reaction with glucose. More specifically, the PBA-modified hydrogel matrix has immobilized cations before binding with glucose, while after binding, both immobilized cations and anionic PBA-glucose complexes exist inside the hydrogel. The charge effect of electron-withdrawing substituents may lead to reduced wavelength shift, although the inductive effect, on the other hand, increases the reactivity of PBAs toward glucose. Although the quantitative evaluation of the charge effect is outside of the scope of our study, it may still play a substantial role in the volumetric change of the PBA-modified hydrogels. Out of the hydrogel matrix, the charge effect of substituents on PBAs does not affect the response, which is not based on the hydrogel volume change.

### 3. CONCLUSION

We investigated the interactions between glucose and PCCAs modified with various PBAs under physiological conditions to elucidate the dependence of the hydrogel's volumetric response on PBA chemistry. For PBAs with boronic acids positioned ortho to the acrylamide linker, a heterocyclic ring is formed that reduces the reaction kinetics of glucose binding and leads to a slow and linear but hysteretic volumetric response of the hydrogel matrix (e.g., 2APBA and 2A5FPBA in Group 1). PCCAs modified with PBAs that do not form the heterocyclic rings show nonlinear but fast response kinetics, with minimal hysteresis. The substituents on PBAs can either increase or decrease the magnitude of response. In terms of response kinetics, introducing electron-withdrawing substituents increases the response rate. Addition of a methylene bridge between the PBA and hydrogel backbone leads to a significant decrease in the response magnitude. pH titration of the PBA-modified PCCAs suggests that the electron-withdrawing substituents may immobilize cationic species and compete with the volumetric change induced by the interactions of PBAs

with glucose, leading to the complication of the wavelength shift during glucose monitoring. To achieve PBA-modified hydrogel systems with linear and fast response and minimal hysteresis, the chemical structure of PBAs and the hydrogel matrix must be engineered to eliminate the effects on volumetric changes by one of the 1:1 and 2:1 PBA–glucose complexes. In addition, PBAs with specific features can be selected from the pool in our study and PBA derivatives with desired properties can be designed according to our findings.

#### 4. EXPERIMENTAL SECTION

**Materials.** Styrene ( $\geq 99\%$ ), divinylbenzene (80%), 3-allyloxy-2-hydroxy-1-propanesulfonic acid sodium salt (40 wt % in  $\text{H}_2\text{O}$ ), dihexyl sulfosuccinate sodium salt (80% in  $\text{H}_2\text{O}$ ), sodium bicarbonate (99.7%–100.3%), ammonium persulfate ( $\geq 98.0\%$ ), inhibitor removers (for removing *tert*-butylcatechol), 3-(trimethoxysilyl)propyl methacrylate (98%), trichloro(1H,1H,2H,2H-perfluorooctyl)silane (97%), acrylamide/bis-acrylamide mixture (AA/BisAA, 37:1 wt ratio), diethoxyacetophenone (DEAP,  $>95\%$ ), mixed bed resin, *N,N,N',N'*-tetramethylethylenediamine (99%), sodium hydroxide (97%), *N*-(3-dimethylaminopropyl)-*N'*-ethylcarbodiimide hydrochloride (EDC, crystalline), D(+)-glucose ( $\geq 99.5\%$ ), phosphate buffered saline tablets, Alizarin Red S (ARS), 2-aminophenylboronic acid hydrochloride (2APBA,  $\geq 95\%$ ), 3-aminophenylboronic acid hemisulfate salt (3APBA,  $\geq 95\%$ ), 4-aminophenylboronic acid hydrochloride (4APBA, 94%), 4-amino-3-fluorophenylboronic acid hydrochloride (4A3FPBA), 4-amino-3-nitrophenylboronic acid (4A3NitroPBA, 90%), and 3-amino-4-methylphenylboronic acid (3A4MethylPBA) were purchased from Sigma–Aldrich. Monopotassium phosphate ( $\geq 99\%$ ), was purchased from Fisher Biotech. 2-Amino-5-fluorophenylboronic acid (2A5FPBA, 96%), 2-amino-4,5-difluorophenylboronic acid (2A45FPBA, 97%), 3-amino-4-fluorophenylboronic acid (3A4FPBA, 96%), 3-amino-5-cyanophenylboronic acid hydrochloride (3A5CyanoPBA, 97%), 3-amino-5-nitrophenylboronic acid hydrochloride (3A5NitroPBA, 96%), 2-amino-4-cyanophenylboronic acid hydrochloride (2A4CyanoPBA, 98%), 2-aminomethyl-4-fluorophenylboronic acid (2Am4FPBA, 97%), 2-aminomethyl-5-nitrophenylboronic acid (2Am5NitroPBA, 96%), 3-aminomethylphenylboronic acid hydrochloride (3AmPBA, 96%), 4-aminomethylphenylboronic acid hydrochloride (4AmPBA, 97%), 2-aminomethyl-5-fluorophenylboronic acid hydrochloride (2Am5FPBA, 98%), 5-aminomethyl-2-fluorophenylboronic acid hydrochloride (5Am2FPBA, 98%), 2-acetylaminophenylboronic acid (2AcePBA, 98%), 3-acetylaminophenylboronic acid (3AcePBA, 98%), and 4-acetylaminophenylboronic acid (4AcePBA, 97%) were purchased from Combi-Blocks. 5-Amino-2-fluorophenylboronic acid (5A2FPBA, 98%) was purchased from Asymchem. All chemicals were used as-received, except where noted.

**Synthesis and Characterization of Highly Charged Monodispersed Polystyrene Colloids.** Highly charged monodispersed polystyrene colloids were synthesized following a reported procedure.<sup>40</sup> In a typical experiment, sodium bicarbonate (0.24 g) was dissolved in Millipore water (200 g) in a three-neck flask. The solution was purged by nitrogen under stirring for 40 min. Dihexyl sulfosuccinate sodium salt solution (2.28 g) was mixed with Millipore water (29 g) and added into the flask and the temperature was increased to 50 °C. A monomer mixture of deinitiated styrene (47.28 g) and divinylbenzene (4.44 g) was added to the reaction system at a rate of 4 mL/min. The 3-allyloxy-2-hydroxy-1-propanesulfonic acid sodium salt solution (15.72 g) was diluted with 12 g of Millipore water and added into the flask 1.5 h after the monomer mixture was added. The temperature was increased to 70 °C. Ammonium persulfate (0.64 g) was dissolved in Millipore water (20 g) and added into the flask. The reaction system was refluxed for 6 h and cooled to room temperature. The resulting polystyrene colloid suspension was purified by dialysis for 30 days until the electrical resistance of the water bath reached the same value as the Millipore water. The purified suspension was condensed in the presence of ion-exchange resin until it showed bright opalescence due to Bragg diffraction of visible light. The concentration of polystyrene colloids is  $\sim 4$  wt %. The colloid

morphology was measured using Hitachi 4800 SEM (see Figure S3 in the Supporting Information). A zeta potential of  $\zeta = -50$  mV was measured with a Malvern Zetasizer.

**Fabrication of PBA-Modified PCCA.** Functionalization of glass substrates was performed according to a reported procedure by our group.<sup>41</sup> Glass slides were cut from microscope slides and cleaned by piranha solution for 2 h. [Warning: Piranha solution is highly oxidative and should be handled following safety guidelines with caution.] Acrylate functionalities were introduced to the bottom slides by treating them with 2 mM 3-(trimethoxysilyl)propyl methacrylate in toluene overnight. Top slides were functionalized in 2 mM trichloro-(1H,1H,2H,2H-perfluorooctyl)silane in chloroform overnight. Both slides were rinsed with ethanol and blown dry by nitrogen. The cell for polymerization consisted of a sandwich structure of a bottom slide, a spacer, and a top slide. Typically, 30- $\mu\text{m}$ -thick spacers (20 mm in diameter) were used. The PCCA thickness is labeled according to the spacer thickness in this paper.

AA/BisAA (0.35 g) and mixed bed resin (0.2 g) were added to CCA (5.0 g). The mixture was shaken on a Vortex mixer for 15 min. A small amount (0.1 g) of DEAP solution (0.1 g DEAP in 1.0 g DMSO) was added, and the resulting polymerization solution was mixed for another 15 min, followed by 5 min of nitrogen purge to remove dissolved oxygen. The nitrogen bubbles trapped in the solution were removed by vacuum. The polymerization solution was taken by a syringe and dropped into a well consisting of the bottom slide and spacer. The top slide was closed carefully to avoid air bubbles and reduce shear force. The sealed cell was clamped and stored in the dark to improve the quality of CCA. The polymerization solution with bright opalescence was polymerized for 2 h using a mercury UV lamp. After polymerization, the top slide was removed carefully and the resulting PCCA attached to the bottom slide was rinsed intensively and equilibrated in water for use.

The PCCA was hydrolyzed in a solution containing 0.16 g of NaOH, 0.35 g of NaCl, 4.0 g of *N,N,N',N'*-tetramethylethylenediamine, and 40 mL of Millipore water at room temperature for various times to introduce different quantities of carboxylic acid groups. PBA derivatives were attached to the hydrolyzed PCCA in 40 mL solution containing 15 mM EDC and 15 mM phenylboronic acid for 30 h at pH 4.8. The PBA-modified PCCA was rinsed with 150 mM NaCl and pH 7.4 buffer before testing.

**Glucose Response Test.** An 18-mL reservoir was attached to the substrate that supports the PBA-modified PCCA, using an epoxy resin. A thin thermocouple was placed immediately above the PCCA top surface to keep the solution at 37 °C. The solution was heated by a heating tape wrapped around the reservoir (Figure 13). During the test, the reservoir was filled with glucose solutions containing 10 mM

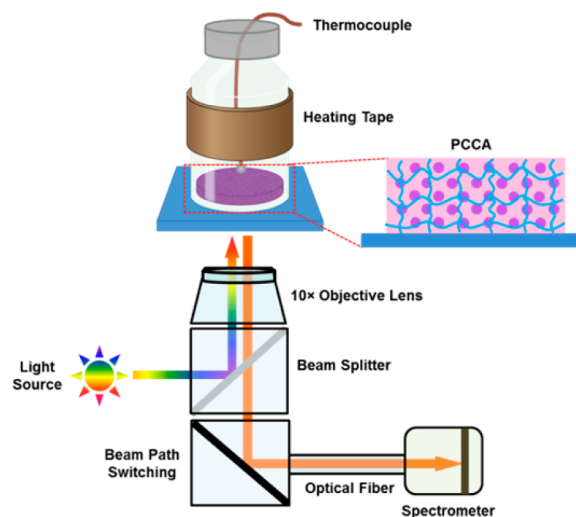


**Figure 13.** Schematic for microspectroscopy of the PBA-modified PCCA.

phosphate, 2.7 mM KCl, and 137 mM NaCl with a pH value of 7.4 (pH 7.4 buffered glucose solutions). The phosphate buffer solution was made by dissolving phosphate buffered saline tablets in Millipore water and the pH was adjusted to 7.4. Glucose solutions were stored over 24 h to reach the mutarotation equilibrium before the test. Reflectance spectra were collected from the bottom side of the PCCA in a normal direction using a 10× objective lens on an inverted optical microscope (Axiovert 135, Carl Zeiss, Inc.). The wavelength range of the spectrometer is 292–1056 nm. The diffraction wavelength in this paper is the reflection maximum by the PCCA.

**Raman Spectroscopy.** Thirty micrometer (30  $\mu\text{m}$ )-thick PAAM hydrogel films of the same composition as the PCCA matrix were hydrolyzed for 70 h and functionalized with different PBAs. The PBA-modified films were first rinsed with DMSO and then Millipore water intensively. Raman spectra were taken from the hydrogel samples dried in air using a Raman confocal imaging microscope with a 532-nm laser and 100× long working distance objective lens (Horiba LabRAM HR 3D). Spectra of AcePBAs were taken on pallets composed of the corresponding AcePBA and KBr.

**UV–vis Spectroscopy.** UV–vis absorbance spectra were collected using a Shimadzu UV-2450 spectrometer. PBA and ARS solutions were made in pH 7.4 buffer and stored overnight before test. The same buffer solution was used as the reference. Quartz cuvettes with 10 mm light path length were used for the measurement.

**pH Titration.** pH titration was performed in a similar way as the glucose response test. The reservoir was filled with ~10 mL of 20 mM  $\text{KH}_2\text{PO}_4$  with pH 4.5. 20mM NaOH (aq) was added dropwise in the reservoir to vary the pH value. The PBA-modified PCCA was allowed to reach equilibrium after the pH value was changed each time. Reflectance spectra were taken at room temperature with a 10× objective lens on an inverted optical microscope (Axiovert 135, Carl Zeiss, Inc.).

## ■ ASSOCIATED CONTENT

### ● Supporting Information

The boron content in bulk hydrogels, equilibrated states of immobilized PBAs, chemical structures of AcePBAs and ARS, and SEM images of the highly charged monodispersed polystyrene colloids are provided in the Supporting Information. This material is available free of charge via the Internet at <http://pubs.acs.org>.

## ■ AUTHOR INFORMATION

### Corresponding Author

\*E-mail: [pbraun@illinois.edu](mailto:pbraun@illinois.edu).

### Present Address

<sup>†</sup>Department of Chemical and Biomolecular Engineering at North Carolina State University, Raleigh, NC 27695, USA.

### Notes

The authors declare no competing financial interest.

## ■ ACKNOWLEDGMENTS

The work was supported by Defense Threat Reduction Agency, under Award No. HDTRA1-12-1-0035, and the University of Illinois at Urbana–Champaign. The authors also want to thank Dr. Scott Robison and Dr. Dianwen Zhang of ITG at Beckman Institute for their technical support.

## ■ REFERENCES

- (1) Wild, S.; Roglic, G.; Green, A.; Sicree, R.; King, H. *Diabetes Care* **2004**, *27*, 1047.
- (2) Wu, Q.; Wang, L.; Yu, H.; Wang, J.; Chen, Z. *Chem. Rev.* **2011**, *111*, 7855.
- (3) Oliver, N. S.; Toumazou, C.; Cass, A. E. G.; Johnston, D. G. *Diabetic Med.* **2009**, *26*, 197.
- (4) Koschinsky, T.; Heinemann, L. *Diabetes/Metab. Res. Rev.* **2001**, *17*, 113.
- (5) Toghill, K. E.; Compton, R. G. *Int. J. Electrochem. Sci.* **2010**, *5*, 1246.
- (6) Pickup, J. C.; Hussain, F.; Evans, N. D.; Rolinski, O. J.; Birch, D. J. S. *Biosens. Bioelectron.* **2005**, *20*, 2555.
- (7) Ravaine, V.; Ancla, C.; Catargi, B. J. *Controlled Release* **2008**, *132*, 2.
- (8) Steil, G. M.; Panteleon, A. E.; Rebrin, K. *Adv. Drug Delivery Rev.* **2004**, *56*, 125.
- (9) Khafagy, E.-S.; Morishita, M.; Onuki, Y.; Takayama, K. *Adv. Drug Delivery Rev.* **2007**, *59*, 1521.
- (10) Ulijn, R. V.; Bibi, N.; Jayawarna, V.; Thornton, P. D.; Todd, S. J.; Mart, R. J.; Smith, A. M.; Gough, J. E. *Mater. Today* **2007**, *10*, 40.
- (11) van der Linden, H. J.; Herber, S.; Olthuis, W.; Bergveld, P. *Analyst* **2003**, *128*, 325.
- (12) Siegel, R. A.; Gu, Y.; Lei, M.; Baldi, A.; Nuxoll, E. E.; Ziaie, B. J. *Controlled Release* **2010**, *141*, 303.
- (13) Kataoka, K.; Miyazaki, H.; Okano, T.; Sakurai, Y. *Macromolecules* **1994**, *27*, 1061.
- (14) Kataoka, K.; Miyazaki, H.; Bunya, M.; Okano, T.; Sakurai, Y. *J. Am. Chem. Soc.* **1998**, *120*, 12694.
- (15) Traitel, T.; Cohen, Y.; Kost, J. *Biomaterials* **2000**, *21*, 1679.
- (16) Holtz, J. H.; Asher, S. A. *Nature* **1997**, *389*, 829.
- (17) Aguirre, C. I.; Reguera, E.; Stein, A. *Adv. Funct. Mater.* **2010**, *20*, 2565.
- (18) Goponenko, A. V.; Asher, S. A. *J. Am. Chem. Soc.* **2005**, *127*, 10753.
- (19) Alexeev, V. L.; Das, S.; Finegold, D. N.; Asher, S. A. *Clin. Chem. (Washington, DC, U.S.)* **2004**, *50*, 2353.
- (20) Steiner, M.-S.; Duerkop, A.; Wolfbeis, O. S. *Chem. Soc. Rev.* **2011**, *40*, 4805.
- (21) Asher, S.; Peteu, S.; Reese, C.; Lin, M.; Finegold, D. *Anal. Bioanal. Chem.* **2002**, *373*, 632.
- (22) Baca, J. T.; Finegold, D. N.; Asher, S. A. *Analyst* **2008**, *133*, 385.
- (23) Ward Muscatello, M. M.; Stunja, L. E.; Asher, S. A. *Anal. Chem.* **2009**, *81*, 4978.
- (24) Xu, X.; Goponenko, A. V.; Asher, S. A. *J. Am. Chem. Soc.* **2008**, *130*, 3113.
- (25) Lee, K.; Asher, S. A. *J. Am. Chem. Soc.* **2000**, *122*, 9534.
- (26) Hall, D. G. *Boronic Acids: Preparation and Applications in Organic Synthesis, Medicine and Materials*; Wiley–VCH: Weinheim, Germany, 2011.
- (27) Nishiyabu, R.; Kubo, Y.; James, T. D.; Fossey, J. S. *Chem. Commun.*, **2011**, 47, 1106.
- (28) Updike, S. J.; Shultz, M. C.; Gilligan, B. J.; Rhodes, R. K. *Diabetes Care* **2000**, *23*, 208.
- (29) Yoon, J.; Cai, S.; Suo, Z.; Hayward, R. C. *Soft Matter* **2010**, *6*, 6004.
- (30) Tokarev, I.; Minko, S. *Soft Matter* **2009**, *5*, 511.
- (31) Asher, S. A.; Alexeev, V. L.; Goponenko, A. V.; Sharma, A. C.; Lednev, I. K.; Wilcox, C. S.; Finegold, D. N. *J. Am. Chem. Soc.* **2003**, *125*, 3322.
- (32) Alexeev, V. L.; Sharma, A. C.; Goponenko, A. V.; Das, S.; Lednev, I. K.; Wilcox, C. S.; Finegold, D. N.; Asher, S. A. *Anal. Chem.* **2003**, *75*, 2316.
- (33) Springsteen, G.; Wang, B. *Tetrahedron* **2002**, *58*, 5291.
- (34) Yang, X.; Lee, M.-C.; Sartain, F.; Pan, X.; Lowe, C. R. *Chem.–Eur. J.* **2006**, *12*, 8491.
- (35) Pan, X.; Yang, X.; Lowe, C. R. *J. Mol. Recognit.* **2008**, *21*, 205.
- (36) Sartain, F. K.; Yang, X.; Lowe, C. R. *Anal. Chem.* **2006**, *78*, S664.
- (37) Smart, B. E. *J. Fluorine Chem.* **2001**, *109*, 3.
- (38) Laurence, C.; Berthelot, M.; Lucon, M.; Morris, D. G. *J. Chem. Soc., Perkin Trans. 2* **1994**, 0, 491.
- (39) Baitinger, W. F.; Schleyer, P. v. R.; Murty, T. S. S. R.; Robinson, L. *Tetrahedron* **1964**, *20*, 1635.
- (40) Reese, C. E.; Guerrero, C. D.; Weissman, J. M.; Lee, K.; Asher, S. A. *J. Colloid Interface Sci.* **2000**, *232*, 76.

(41) Lee, Y.-J.; Pruzinsky, S. A.; Braun, P. V. *Langmuir* **2004**, *20*, 3096.